Research Square

Preprints are preliminary reports that have not undergone peer review.
They should not be considered conclusive, used to inform clinical practice,
or referenced by the media as validated information.

Mobility-weighted heat exposure reveals priority corridors for climate-resilient cycling

Ferdinand Briegel
Karlsruhe Institute of Technology
Ariane Middel
ariane.middel@asu.edu
Arizona State University
Andreas Christen
University of Freiburg

Article

Keywords: urban overheating, active mobility, cycling infrastructure, heat exposure, tree canopy, nature-based solutions, urban climate informatics

Posted Date: November 25th, 2026

DOI: https://doi.org/10.21203/rs.3.rs-11639181/v1

License: This work is licensed under a Creative Commons Attribution 4.0 International License.
Read Full License

Additional Declarations: No competing interests reported.

Mobility-weighted heat exposure reveals priority corridors for climate-resilient cycling

FERDINAND BRIEGEL
Institute of Meteorology and Climate Research - Troposphere Research (IMKTRO)
Karlsruhe Institute of Technology, Karlsruhe, Germany
Hermann-von-Helmholtz-Platz 1, 76344 Eggenstein-Leopoldshafen
ferdinand.briegel@kit.edu

ARIANE MIDDEL*
The GAME School, School of Geographical Sciences and Urban Planning
Arizona State University, USA
University of Freiburg
950 S. Forest Mall, Stauffer B258
Tempe, AZ 85281
ariane.middel@asu.edu

ANDREAS CHRISTEN
Chair of Environmental Meteorology
Faculty of Environment and Natural Resources
University of Freiburg
Werthmannstrasse 10
79085 Freiburg im Breisgau
andreas.christen@meteo.uni-freiburg.de

*Correspondence concerning this article should be addressed to Ariane Middel, The GAME School, 501 E Orange St., Tempe, AZ 85281, Arizona State University; e-mail: ariane.middel@asu.edu

Abstract (150 words)

Urban overheating threatens efforts to expand low-carbon active mobility, yet cities lack scalable methods to identify where heat most affects cyclists. This study integrates high-resolution biometeorological modeling with segment-based cycling mobility data to distinguish between heat hazard and actual heat exposure. Using a building and tree-resolving machine-learning model (HTC-NN), hourly Universal Thermal Climate Index rasters are generated at 1 m spatial resolution for Freiburg, Germany, during a summer cycling campaign in 2023. Recorded cycling activity data are used to estimate the cumulative exposure cyclists experience along cycling segments. Results show substantial intra-urban variability in heat hazard, but exposure patterns differ when accounting for cyclist activity. Heavily used corridors produced high exposure even under moderate hazard. Existing tree canopy reduced cumulative cyclist heat exposure by 29%, with benefits depending on shade, urban form, and cycling activity. This framework supports targeted, climate-resilient active transport planning.

Keywords: urban overheating; active mobility; cycling infrastructure; heat exposure; tree canopy; nature-based solutions; urban climate informatics

Abbreviations

CET	Central European Time
CHEH	Cumulative Heat Exposure Hours (for the 3 weeks) [Unit h/km]
CHHH	Cumulative Heat Hazard Hours (for the 3 weeks) [Unit h]
DSM	Digital Surface Model
DWD	German Meteorological Service (Deutscher Wetterdienst)
HEH	Heat Exposure Hours (on hourly resolution) [Unit h/km]
HHH	(fractional) Heat Hazard Hours (on hourly resolution, between 0 and 1) [Unit h]
HTC-NN	Human Thermal Comfort Neural Network
HS	Heat Stress
MRT	Mean Radiant Temperature
PET	Physiologically Equivalent Temperature
UTCI	Universal Thermal Climate Index

1. Introduction

Cities are central to the sustainability transition, but they are also increasingly exposed to climate risks that threaten public health, mobility, and everyday urban life. Urban overheating has emerged as one of the most pressing challenges for cities worldwide[1]. Rising air temperatures and more frequent, intense heatwaves are becoming increasingly evident[2], trends that are particularly pronounced in cities, where the urban heat island effect exacerbates thermal conditions through interactions among built surfaces, limited vegetation, and reduced nocturnal cooling[3]. Consequently, urban environments frequently experience greater and more prolonged heat stress than their rural surroundings[4]. These conditions pose a direct challenge to sustainable urban development by reducing outdoor livability, discouraging active travel, increasing health risks, and undermining efforts to shift cities toward low-carbon mobility systems. This intensification has far-reaching implications for public health, urban livability, and how people use and move through cities[5].

A growing body of research has therefore focused on identifying where and when heat stress occurs within cities [1]. Over time, assessment approaches have evolved from air temperature-based metrics to more physiologically meaningful indicators, such as mean radiant temperature (MRT)[6,7], the Physiologically Equivalent Temperature (PET)[8], and the Universal Thermal Climate Index (UTCI)[9]. Biometeorological indices offer a more comprehensive representation by integrating multiple atmospheric variables into a single measure of thermal stress[10,11]. In parallel, the analytical focus has shifted from broad characterizations of the urban heat island to high-resolution assessments of intra-urban thermal variability, revealing pronounced differences in heat stress at the street scale[12–14].

However, these advances have primarily improved our understanding of heat as a hazard, rather than the actual exposure experienced by urban populations. Heat hazard describes the spatial and temporal distribution of potentially harmful thermal conditions (e.g., critical heat stress thresholds), independent of human activity[15]. In contrast, heat exposure depends on where and when people are present and moving through the city[16,17]. As a result, areas with high modeled heat stress do not necessarily correspond to locations where population density and, hence, exposure are greatest. Adaptation resources may be

misallocated if cities prioritize thermally extreme locations without considering whether people use those spaces, when they use them, and who benefits from mitigation. Although high-resolution environmental data can identify hotspots of heat hazard[18], a realistic assessment of heat exposure requires integrating hazard and mobility data.

Active mobility illustrates this challenge especially well. Cycling is a low-carbon, space-efficient, and health-promoting mode of transport, and is therefore central to many urban sustainability strategies[19,20]. At the same time, cycling is uniquely sensitive to environmental conditions[21]. Unlike users of motorized transport, cyclists are exposed to atmospheric conditions, and their travel behavior depends on a combination of meteorological factors[22–24] and characteristics of the urban environment[25]. Previous studies have shown that cycling activity increases with air temperature up to a threshold beyond which participation declines[26,27]. Thus, urban heat can create a sustainability trade-off: cities aim to increase cycling to reduce emissions and support healthier lifestyles, yet rising heat may make cycling less safe and less comfortable. This underscores the need to better understand and mitigate heat exposure along cycling routes.

Heat exposure varies continuously along routes, depending on street orientation, surrounding buildings and vegetation, and the time of day[28,29]. Consequently, the impact of heat on cycling cannot be fully understood using aggregated or location-independent measures[30,31]. Most existing research on the interaction between cycling and urban heat has relied on stationary meteorological data combined with cyclist counts or bike-sharing usage. More recent work has begun to incorporate sshading, demonstrating that shaded cycling infrastructure is associated with increased cycling activity[32,33]. While these studies represent an important step toward linking environmental conditions and behavior, they typically remain unidirectional, using environmental variables to explain mobility patterns without explicitly quantifying cyclists' thermal exposure. Similarly, studies that incorporate mobility modeling approaches, such as the ICARUS model[34,35], capture how environmental conditions influence movement patterns, but do not explicitly couple these dynamics with high-resolution biometeorological conditions to assess how exposure evolves in response to both environment and behavior. As a result, cities still lack scalable methods for

identifying where heat most threatens active mobility and where adaptation interventions would provide the greatest collective benefit.

Urban form plays a decisive role in shaping heat hazard and exposure. Vegetation, especially street trees, can substantially alter street-level microclimates[36,37]. By providing shade, trees reduce incoming shortwave radiation and MRT, which are key drivers of human heat stress outdoors[38,39]. This can lead to significant reductions in perceived heat, even when air temperature remains unchanged[40,41]. Urban trees and shaded streets are therefore not only local cooling measures, but also nature-based infrastructure that can support climate resilience, public health, and sustainable mobility. However, the effectiveness of tree canopy in mitigating heat exposure along mobility networks depends strongly on its spatial configuration relative to solar position and travel paths, street geometry, and surrounding buildings[42]. While previous studies have quantified the cooling effects of vegetation at neighborhood or city scales[43,44], fewer have examined how tree shade influences actual exposure experienced along frequently used cycling routes. This represents a critical knowledge gap for climate-resilient transport planning, because the sustainability value of urban greening depends not only on where trees reduce heat, but also on whether those reductions occur where and when people are exposed.

Recent advances in urban climate informatics enable addressing this gap by linking high-resolution environmental models with digital traces of urban activity[45]. High-resolution biometeorological models, including machine learning approaches, enable rapid simulation of thermal comfort maps (UTCI) at the building levels[14,46]. Meanwhile, GPS-based mobility datasets allow detailed reconstruction of recorded movement patterns across urban cycling networks. Combining these data sources enables a shift from mapping where heat occurs to understanding how heat is experienced in relation to human mobility and activity. Such data-integrated approaches are particularly relevant for urban sustainability because they can translate complex climate-risk information into actionable evidence for infrastructure prioritization, nature-based solutions, and adaptation planning.

We integrate these approaches by combining segment-based cycling data[47] with high-resolution biometeorological modeling[14] in the City of Freiburg, Germany. Cycling activity is derived from GPS-

tracked records collected during a city-wide campaign, providing anonymized, aggregated information at the level of individual street segments, including hourly activity counts, average speeds, and segment lengths. These data are linked to meter-scale UTCI raster data generated at hourly resolution for the entire urban area using a machine-learning-based model. This coupling provides a detailed representation of thermal conditions along all recorded cycling routes over time. Furthermore, by simulating scenarios with and without tree canopy, the influence of vegetation on thermal perception and heat stress can be explicitly isolated and quantified. Rather than treating heat mitigation as a purely biophysical problem, our approach evaluates mitigation in relation to observed mobility, allowing us to distinguish places that are thermally hazardous from places where cyclists are exposed.

Based on this integrated framework, the study has three main objectives: (i) to develop and apply a scalable exposure-based framework that combines high-resolution urban climate modeling with crowdsourced mobility data; (ii) to distinguish heat hazard from cyclist heat exposure across an urban cycling network; and (iii) to assess how existing tree canopy contributes to heat-risk reduction for active mobility. Using the City of Freiburg as a case study, the analysis provides transferable insights into how climate risk, urban form, nature-based cooling, and mobility patterns interact in sustainable urban systems. The study contributes to urban sustainability research by showing how digital mobility data and microclimate modeling can support more targeted, evidence-based, and climate-resilient planning of active transport infrastructure.

2. Results

We quantify cyclists' thermal risk using two complementary metrics that distinguish heat as an environmental condition from heat as an experienced mobility burden. Cumulative heat hazard hours (CHHH) describe how often each cycling segment exceeds UTCI heat-stress thresholds, independent of whether cyclists are present. Cumulative heat exposure hours (CHEH) weight these thermal conditions by observed cycling activity and travel speed, thereby estimating where heat is most likely to affect cyclists in practice. Unless stated otherwise, results focus on strong heat stress or higher (UTCI > 32 °C) during daytime cycling hours from 08:00 to 22:00 h CET over the 20-day summer campaign.

2.1 Heat hazard varies substantially across the cycling network

The average cumulative heat hazard hours (CHHH) of the used cycling paths over the three weeks are shown in **Table 1** and **Figure 1**. On average across all segments, moderate heat stress (32 °C > UTCI > 26 °C) lasted 89.5 hours, and strong heat stress (38 °C > UTCI > 32 °C) lasted 57.1 hours. Very strong heat stress (46 °C > UTCI > 38 °C) occurred less frequently, averaging 13.0 hours. **Figure 1b** presents a histogram of CHHH with UTCI values exceeding 32 °C for all segments, indicating considerable variability ranging from 0 to more than 100 hours over the study period. The intra-urban spatial variability of CHHH across segments within the city of Freiburg does not reveal a clear spatial pattern associated with urban or rural settings. Rather, it indicates fewer CHHH in the city center and in the eastern part of the city, which lies along mountain slopes, and more CHHH in the western parts. The former are characterized by neighborhoods dating from the early 1900s with large, mature trees, while the latter are characterized by wider streets and partially industrial areas with a younger tree population.

Table 1: Average values of UTCI and cumulative heat hazard hours of each segment for the three weeks and for the different stress classes. HS is heat stress.

		Cumulative heat hazard hours (CHHH) (h)		
	UTCI (°C)	**Moderate HS**	**Strong HS**	**Very strong HS**
Mean	27.1 (± 1.1)	89.5	57.1	13.0
Maximum	41.5 (± 2.2)	132.4	102.1	30.2

Minimum	14.7 (± 1.9)	0.8	0.4	0.0

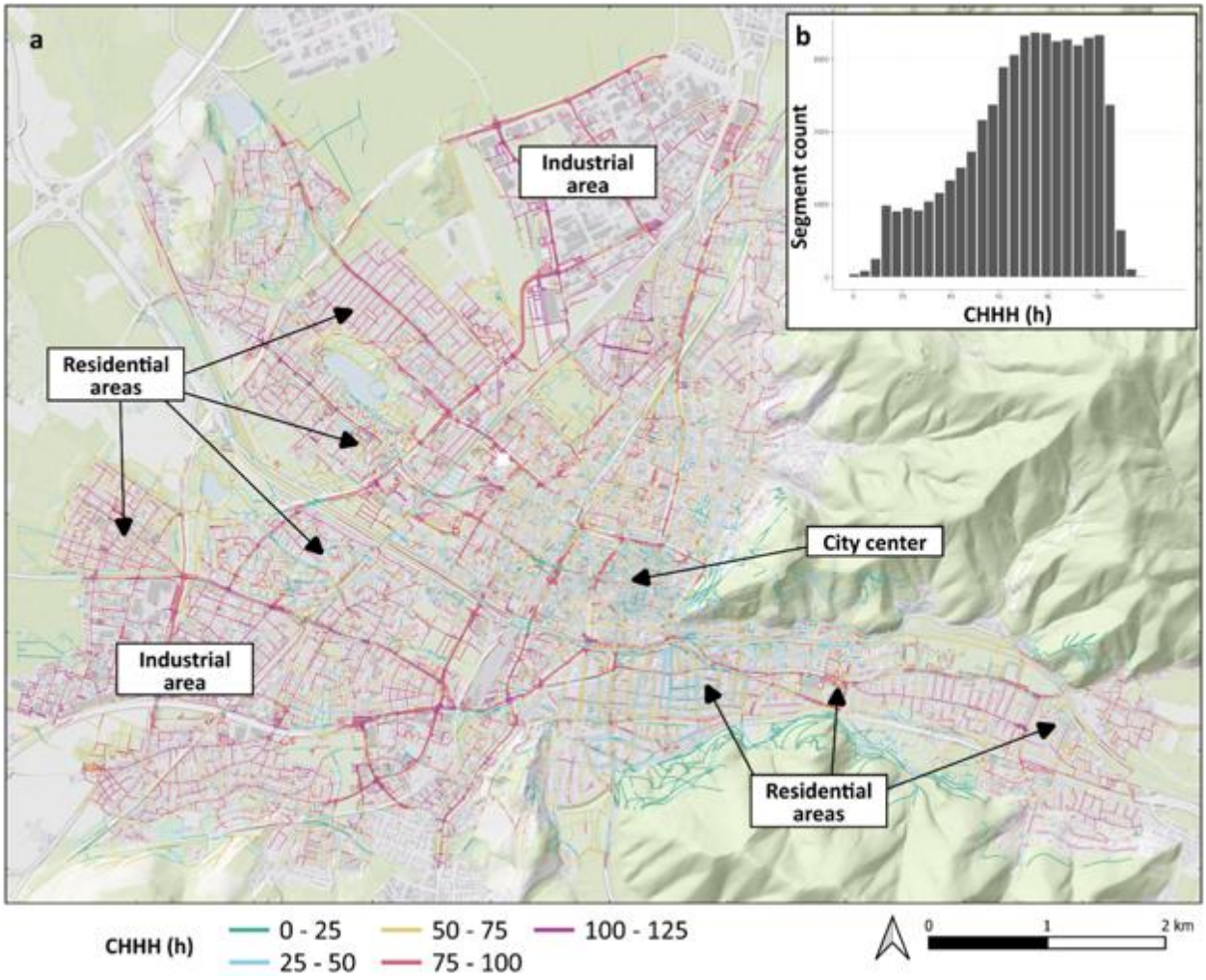


Figure 1: Cumulative heat hazard hours (CHHH) for UTCI > 32 °C reflecting strong heat stress or higher over the three-week study period depicted as a map (a) and as a histogram (b).

2.2 Cumulative Heat Exposure Hours

2.2.1 Spatial Variability

The actual cumulative heat exposure hours (CHEH) experienced by cyclists are estimated based on the number of cyclists, the average cycling speed, and the respective HHH. **Figures** 2a and 2c illustrate the distribution of CHEH in the current state and in a scenario without the existing tree canopy, respectively, while **Figures** 2b and 2d show the corresponding spatial distributions of CHEH. In both scenarios, CHEH

ranges from 0 to over 5500 h km^{-1}. This wide range is due to differences in average cycling speed and the number of cyclists recorded per segment and hour.

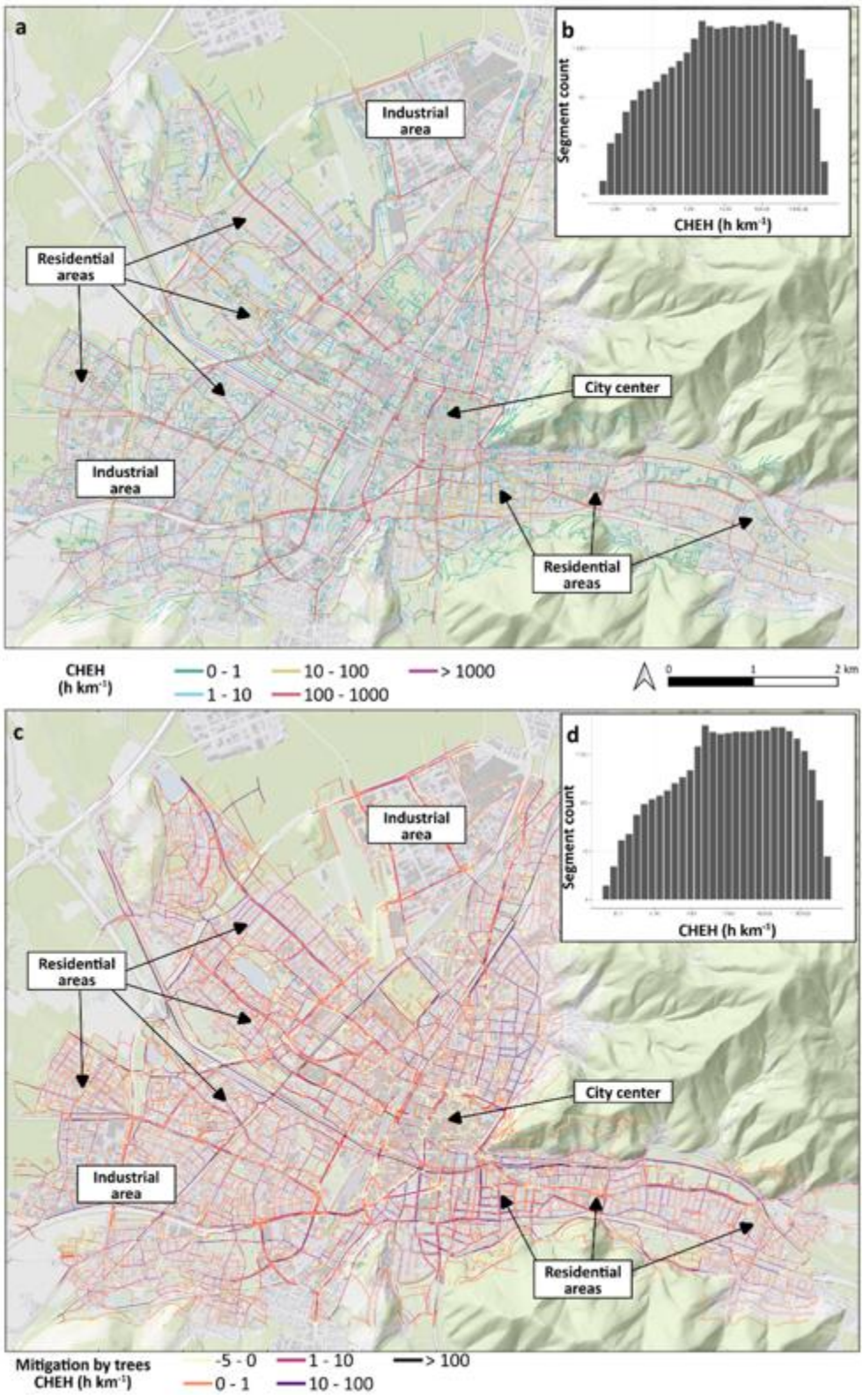


Figure 2: Cumulative heat exposure hours (CHEH) per km for each segment for the three weeks for strong heat stress depicted as a map (a) and a histogram (b) for the current state. The second row (c, d) shows the mitigation potential of the current tree canopy. Note that both axes are logarithmic in (b) and (d).

The intra-urban spatial distribution of CHEH does not exhibit a distinct pattern that can be directly attributed to urban morphology or tree cover. It generally corresponds to the spatial distribution of CHHH, with higher values along frequently used bike lane segments. While the exposure of individual bike lanes appears to affect the calculated heat hazard and the resulting CHEH, the inclusion of cyclist counts partly masks the underlying hazard signal. Consequently, segments with high traffic volumes show pronounced differences in CHEH, as seen in the city center and its southern areas.

Figure 2c does not clearly show a spatial pattern of heat mitigation by the existing tree cover, though neighborhoods in the city's southeastern part tend to exhibit greater mitigation. CHEH averaged across all segments over the three weeks amounts to 133 h km^{-1} in the current state and 173 h km^{-1} in the no-tree scenario. This corresponds to an average 29% reduction in cyclists' heat exposure due to Freiburg's existing tree cover. However, this aggregated mitigation effect likely masks substantial small-scale variability, as the reduction in CHEH depends strongly on the specific shading conditions of individual street segments. A more detailed assessment of the relationship between street-level vegetation and the built environment is required to better understand the drivers of heat exposure and its mitigation.

2.2.2 Temporal Variability of Heat Hazard and Exposure Hours

The temporal variability of HHH and HEH shows a clear diurnal pattern (Figure 3a). HHH increases in the morning, peaking between 13:00 h and 16:00 h, with a local minimum at 14:00 h. This local minimum in HHH occurs shortly after the peak in downward shortwave radiation, which reaches its maximum at 13:00 h before decreasing (**Figure 3c**). In contrast, air temperature continues to increase until around 17:00 h. After 16:00 h, HHH decrease rapidly towards evening. Hourly HEH,

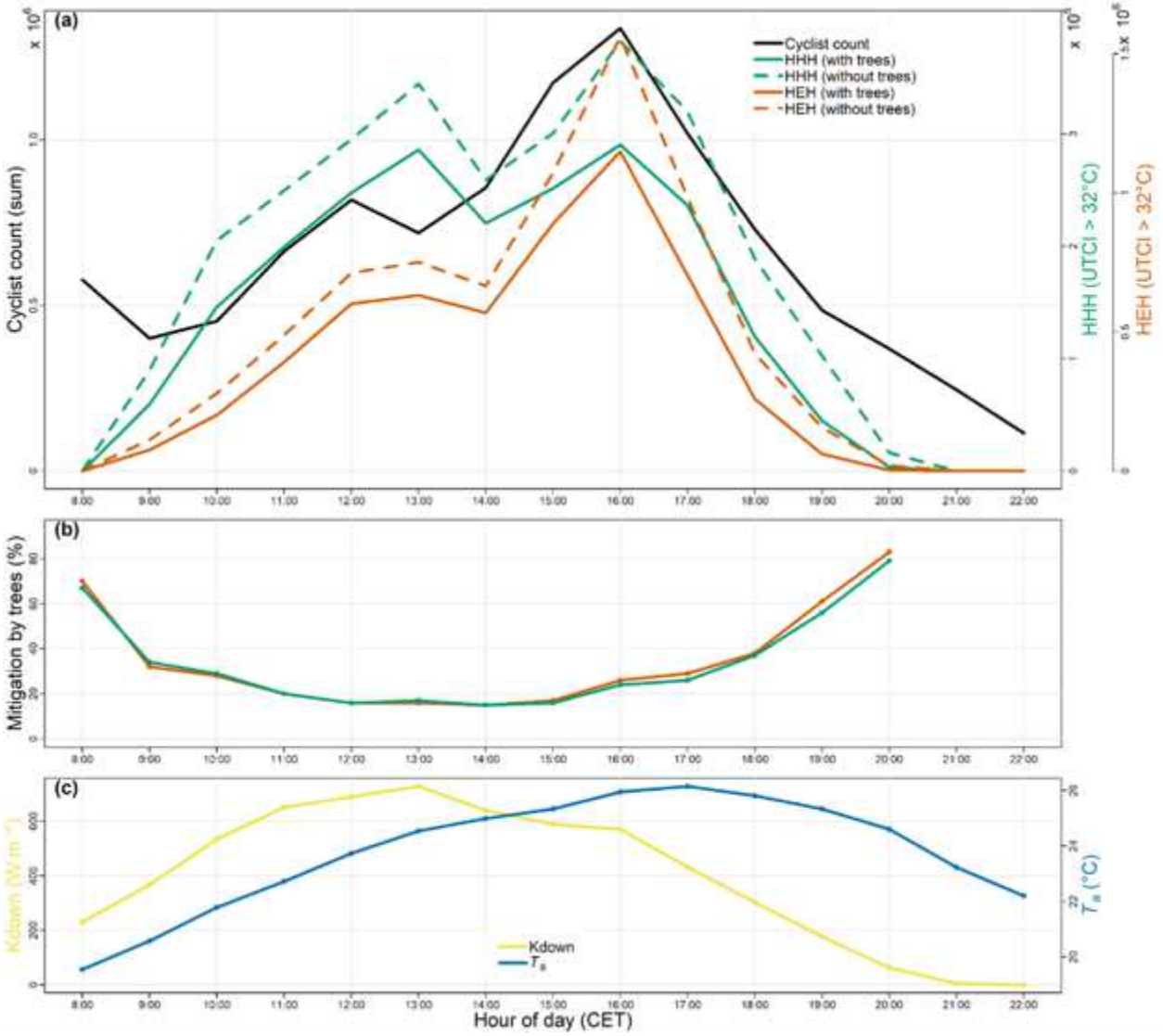


Figure 3: Diurnal cycle of counted cyclists, hourly heat hazard hours (HHH), and hourly heat exposure hours (HEH) of weekdays for the current state and the scenario without trees (a). The average mitigation potential of the current tree canopy is shown in (b) for heat hazard and exposure. Average diurnal cycles for downward shortwave irradiance (Kdown) and air temperature (T_a) are shown in (c).

however, exhibits a different diurnal pattern, with HEH increasing throughout the day and peaking at 16:00 h, which coincides with the peak in cyclist counts.

The presence of tree cover reduces both HHH and HEH throughout the day (**Figures 3a and 3b**). Relative reductions vary over the diurnal cycle. At midday, the reductions are approximately 20% for HHH and for HEH. Higher relative reductions occur during the morning and evening, with reductions of over 60% in the early morning and up to 80% in the evening.

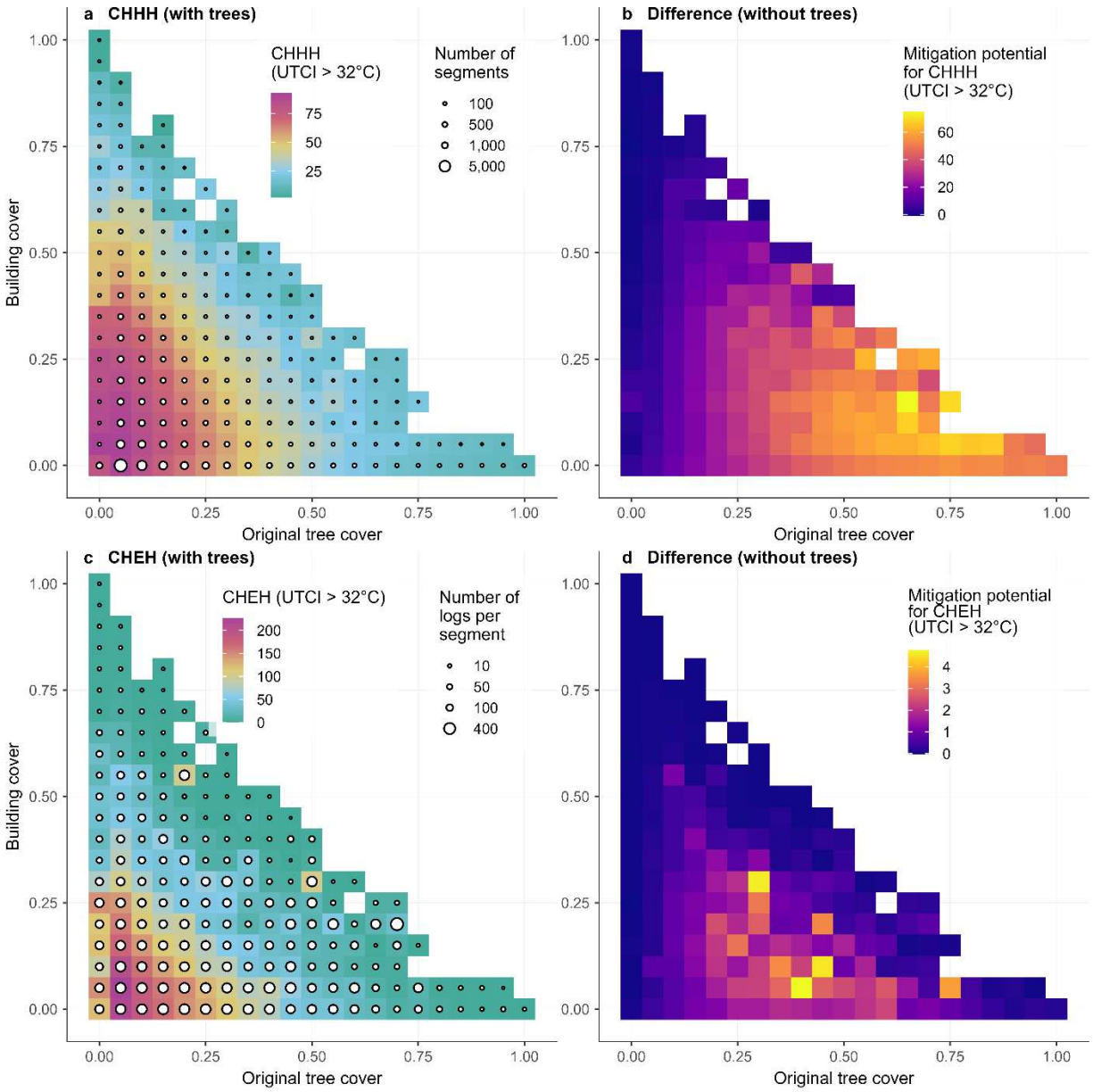


Figure 4: The average cumulative heat hazard hours (CHHH) per segment over the entire three-week period as a function of building and tree cover for the actual case (a) with tree coverage, and the potential for reducing CHHH through the existing tree canopy (b). Subplots (c) and (d) show the results for cumulative heat exposure hours (CHEH), which takes the actual occurrence of cyclists and their speed into account.

2.3 Role of Shade from Trees and Urban Infrastructure

CHHH and CHEH clearly depend on the combination of tree and building cover (**Figure 4**). The highest number of CHHH occurs in areas with low levels of both tree and building cover. As tree cover increases, CHHH decreases across all levels of building cover. A similar reduction is observed with increasing

building cover at low levels of tree cover. Locations characterized by high levels of tree and building cover exhibit the lowest CHHH. The mitigation potential of trees varies across the urban morphology space defined by tree and building cover. The greatest difference in CHHH between the scenario with and the scenario without trees is found in areas with intermediate to high tree cover and low building cover. In contrast, the difference is lower in areas with little tree cover. A minimum of 15%–20% tree cover is needed to substantially reduce heat hazard on cycling lanes.

A comparable pattern is observed for CHEH (**Figure 4c**). The highest values occur in areas with low to medium tree and building cover. In addition, CHEH is strongly influenced by the average number of logs per segment, which is higher in neighborhoods with low- to medium-rise buildings and tree cover (0%–25% and 0%–40%, respectively). The spatial variability of the difference of CHEH between the tree and no tree scenario differs from that observed for CHHH (**Figure 4d**). The largest differences are found at intermediate levels of tree cover (25%–50%) and low to moderate building cover (5%–20%), with some strong outliers. In contrast, areas with very low or very high levels of tree cover have comparatively smaller differences. A case study for selected road segments in Freiburg is presented in Supplemental Materials.

3. Discussion

3.1 Mobility weighting reshapes heat-risk priorities

This study shows that heat risk for active mobility cannot be inferred solely from thermal hazard maps. By combining high-resolution UTCI modeling with observed cycling activity, we distinguish where thermally stressful conditions occur from where cyclists are most likely to experience them. This distinction changes the interpretation of urban heat risk. Segments with high cumulative heat hazard were not always the segments with the greatest cumulative cyclist exposure, while heavily used corridors emerged as exposure hotspots even under moderate thermal conditions. This finding extends previous work on urban heat exposure and vulnerability, which emphasizes that risk depends not only on the spatial distribution of hazard but also on the presence, movement, and characteristics of exposed populations[48–50]. For climate-

resilient cycling planning, this means the most relevant intervention locations are not necessarily the hottest parts of the city, but rather where heat and cycling activity overlap most strongly.

The difference between heat hazard and heat exposure reflects the interaction between microclimate, mobility patterns, and time. The spatial variability of cumulative heat hazard hours in Freiburg is shaped by urban morphology, consistent with previous work showing strong intra-urban variability in thermal conditions at fine spatial scales[51–53]. Heat hazard followed a diurnal meteorological cycle, increasing throughout the morning and peaking in the early afternoon. Heat exposure peaked later, coinciding with elevated thermal conditions and higher cycling activity. This temporal mismatch is important for sustainable transport planning because the periods of greatest collective exposure may differ from the periods of greatest environmental hazard. Infrastructure interventions should therefore be evaluated not only by their capacity to reduce thermal stress at midday, but also by their ability to reduce exposure during high-use periods.

Our findings extend prior research on cycling and heat. Many earlier studies relied on stationary meteorological observations or aggregated weather variables to explain cycling demand, ridership, or bike-share activity[54–59]. These studies have been important in showing that cycling behavior responds to weather and declines under unfavorable thermal conditions, but they do not resolve the heat burden encountered along specific routes. More recent work has incorporated environmental characteristics such as shade, demonstrating that shaded cycling infrastructure is associated with increased cycling activity[60,61]. These approaches generally remain explanatory rather than exposure-based: they use environmental variables to interpret mobility patterns, but do not explicitly quantify the biometeorological exposure experienced by cyclists. Our approach complements and extends these works by integrating high-resolution thermal conditions with observed mobility at the segment level.

The results also relate to mobility modeling studies such as those by Li et al.[62,63], which examine how environmental conditions influence movement behavior and traveler heat exposure. These studies are important for understanding behavioral adaptation and transport-system responses to heat, but they do not explicitly couple observed cycling activity with street-scale biometeorological conditions. The present

framework addresses this gap by linking crowdsourced cycling activity with hourly, meter-scale UTCI rasters. Although it does not yet model adaptive route choice under heat, it provides a more realistic representation of experienced exposure than hazard mapping alone.

3.2 Tree benefits depend on urban form and cycling behavior

The results further demonstrate that tree canopy can substantially reduce heat exposure for cyclists, but that its benefits are spatially uneven. Existing tree canopy reduced cumulative cyclist heat exposure by 29% across the network, confirming the value of urban trees as nature-based infrastructure for heat-resilient active mobility. This finding aligns with previous studies showing that trees and shade reduce shortwave radiation, mean radiant temperature, and outdoor thermal stress[64–66]. It also supports broader evidence that vegetation can modify urban microclimates and improve outdoor thermal comfort, although cooling effects vary with background climate, urban morphology, and tree characteristics[67–70]. In our study, the largest exposure reductions occurred where tree shade, surrounding urban form, and cyclist activity aligned. Segments with substantial canopy but little cycling activity contributed less to collective exposure reduction, while highly used but weakly shaded corridors remained exposure priorities. This finding highlights an important planning implication: urban greening strategies designed for heat adaptation should not be evaluated only by canopy area or local cooling potential, but also by whether shade is located where and when people move through the city.

3.3 Implications for climate-resilient cycling planning

Buildings and urban form further shaped thermal conditions along the cycling network. Higher building cover was associated with lower heat hazard in some contexts, likely due to shading, but the effect depended on local geometry, orientation, and the interaction with vegetation. This is consistent with prior work showing that street design parameters, aspect ratio, orientation, and surrounding urban form strongly influence human-biometeorological conditions[51,71]. The corridor-scale analysis, therefore, suggests that heat-resilient cycling infrastructure requires an integrated view of street design, tree placement, surrounding built form, surface characteristics, and mobility demand. This is particularly relevant for cities seeking to expand cycling as a low-carbon mode of transport[72,73]. Without attention to thermal exposure, efforts to

promote active mobility may be undermined by rising heat, especially during summer conditions and future heatwaves. Conversely, targeted shading along high-use corridors can support both climate adaptation and transport decarbonization by making cycling safer and more comfortable.

Our framework contributes to urban sustainability research by linking digital mobility traces with high-resolution urban climate modeling. Crowdsourced cycling data provide a scalable way to represent where and when active travel occurs, while microclimate modeling resolves the strong spatial variability in outdoor heat stress created by vegetation, buildings, surface characteristics, and atmospheric forcing. This approach builds on recent advances in urban climate informatics, which emphasize the use of data-intensive and computational methods to understand urban climate processes and support decision-making[74]. Combining these data sources allows cities to move from hazard-based hotspot mapping toward exposure-based infrastructure prioritization. This can support decisions about where to preserve mature canopy and prioritize new tree planting or artificial shade. Although the present application focuses on Freiburg, the workflow is transferable to other cities where mobility, urban form, and meteorological data are available.

3.4 Limitations and future directions

Several limitations should be considered when interpreting the results. First, the mobility data are aggregated at the segment level and do not allow reconstruction of individual trajectories, trip purposes, or repeated exposure for specific cyclists. Second, the STADTRADELN data represent a voluntary sample of cycling activity and may not fully capture all cyclist groups or trip types, even though scaling with stationary count data provides an estimate of total activity. Third, cyclist behavior is treated as observed rather than dynamically responsive to heat. Cyclists may avoid hotter routes, shift trips to cooler times of day, reduce trip frequency, change speed, or choose other modes during hot conditions. Fourth, the exposure metrics do not account for differences in physiological vulnerability or heat sensitivity. UTCI provides a standardized measure of outdoor thermal stress, but older adults, children, people with pre-existing health conditions, and cyclists with varying fitness or acclimatization may experience the same thermal conditions differently[49,75]. Finally, the HTC-NN-modeled UTCI values contain uncertainty. Although the model has been validated for Freiburg and performs well relative to sensor network observations and numerical model

outputs[53,76], uncertainty remains particularly relevant near heat-stress thresholds and in locations with complex shading patterns. Future work should propagate model uncertainty through exposure metrics, combine mobility data with demographic or survey data, and develop coupled heat–mobility models that capture behavioral adaptation.

Despite these limitations, the findings show that integrating microclimate modeling with mobility data provides a more actionable basis for heat-resilient active transport planning than hazard mapping alone. As cities seek to reduce emissions, expand active mobility, and adapt to intensifying heat, exposure-based approaches can help identify where nature-based cooling and infrastructure investments are most likely to protect cyclists and sustain low-carbon urban mobility.

4 Methods

4.1 Study Area and Analysis Period

Freiburg im Breisgau (47.995°N, 7.850°E), situated in the Upper Rhine Valley on the western edge of the Black Forest, is one of Germany's warmest and sunniest cities (Figure 6). According to the Köppen climate classification system, its climate is classified as *Cfb*, characterized by mild winters, warm summers, and evenly distributed precipitation of around 886 mm per year[77]. The city's average annual air temperature has risen to around 11.0 °C, with an increasing number of hot days (above 30 °C) and tropical nights, reflecting regional climate warming. Due to its topography and dense urban structure, Freiburg experiences a notable yearly urban heat island effect of on average 2 K. Measurements report up to 30 tropical nights per year in the city center[78]. Ongoing climate change is expected to intensify summer heat waves and droughts in Freiburg[79].

The study period runs from June 19 to July 8, 2023, and is defined by the availability of cyclist mobility data. During the study period, air temperatures in the city center averaged 22.0 °C and ranged from 12.8 °C to 32.6 °C. The period spans five days during which the German Meteorological Service issues official heat warnings[80]. The period June 19 to July 8, 2023, was substantially warmer (+1.04 K) and slightly sunnier (solar irradiance +3%) compared to the long-term climatology for the same days across all years 2020–2025[81]. There was substantial rainfall on 8 of the 20 days during the study period, totaling 63 mm, primarily from convective precipitation. The most notable is June 30, with 26 mm per day.

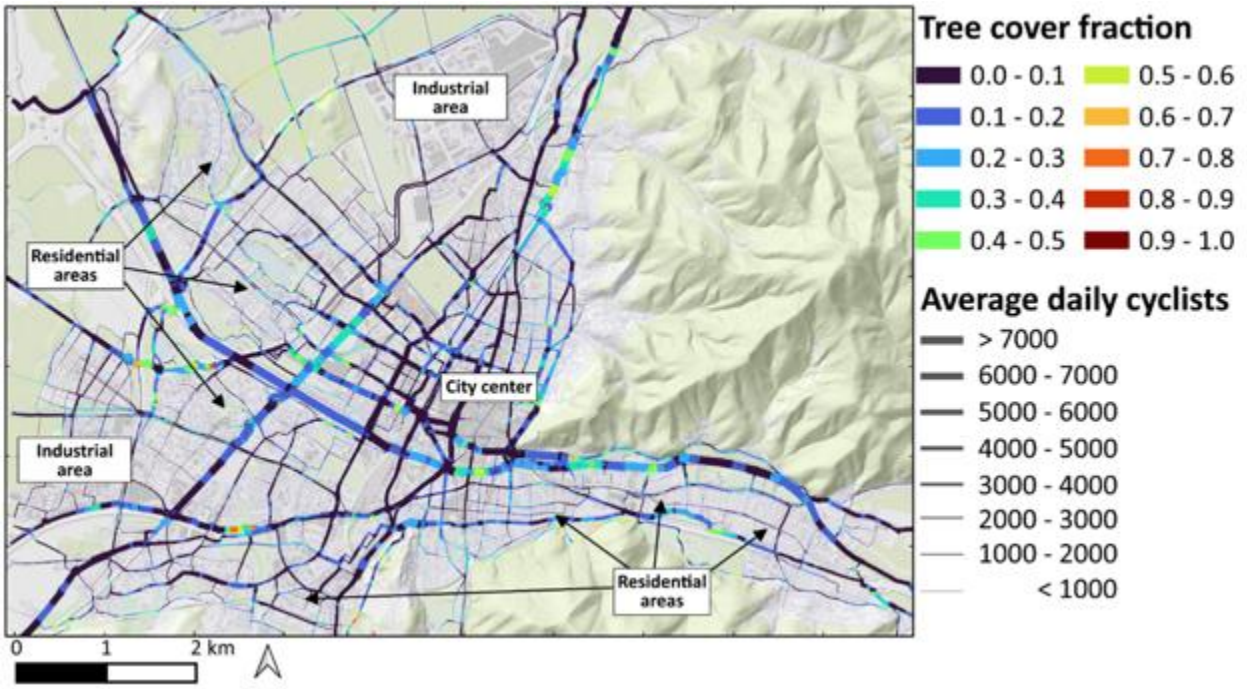


Figure 6: Study area with segments, cycling volume per day (line thickness), and tree canopy cover fraction of the segments (color).

4.2 Cycling Mobility Data

Mobility data are available from a crowd-sourced event called 'STADTRADELN' (engl. 'City Cycling') – a nationwide initiative in Germany organized by the Climate Alliance (Klima-Bündnis) to promote cycling as a sustainable, climate-friendly mode of transport[47]. During the 20-day event each year, participants record their commuting and recreational cycling routes via a GPS-tracked app to encourage low-carbon mobility, raise environmental awareness, and inform improvements to local cycling infrastructure. From this event, anonymized and aggregated hourly data are provided at the spatial level of individual street segments, defined by OpenStreetMap segment IDs. The anonymized data outcomes of the 'STADTRADELN' project include the total number of participants, the average speed, and the number of reported logs (cyclists) per segment at an hourly resolution. In 2023, Freiburg recorded 9281 active participants who cycled approximately 2.2 million kilometers over 20 days[47]. Since this study focuses on daytime heat exposure, and nocturnal data have lower cyclist counts and are generally less significant for

heat exposure, only records from 08:00 h to 22:00 h (CET) are used. A total of 51,363 cycling activity segments are recorded, ranging in length from 0.1 to 650 meters (Figure 7). As not all active cyclists in the city and region are participating in this campaign, the campaign data do not represent the total number of cyclists during the study period. However, Freiburg has multiple stationary cyclists counting stations along main cycling routes that count all cyclists passing by using embedded induction loops in the street, providing an estimate of the total number of cyclists and, consequently, the total impact. Station counts show that only 2.7% of cyclists are recorded by the 'STADTRADELN' campaign and app, suggesting the actual number of cyclists and the overall heat impact on cyclists are likely to be around $s = 1/0.027 = \sim 37$ times greater than the results estimated by the 'STADTRADELN' campaign. Hence, all values shown in

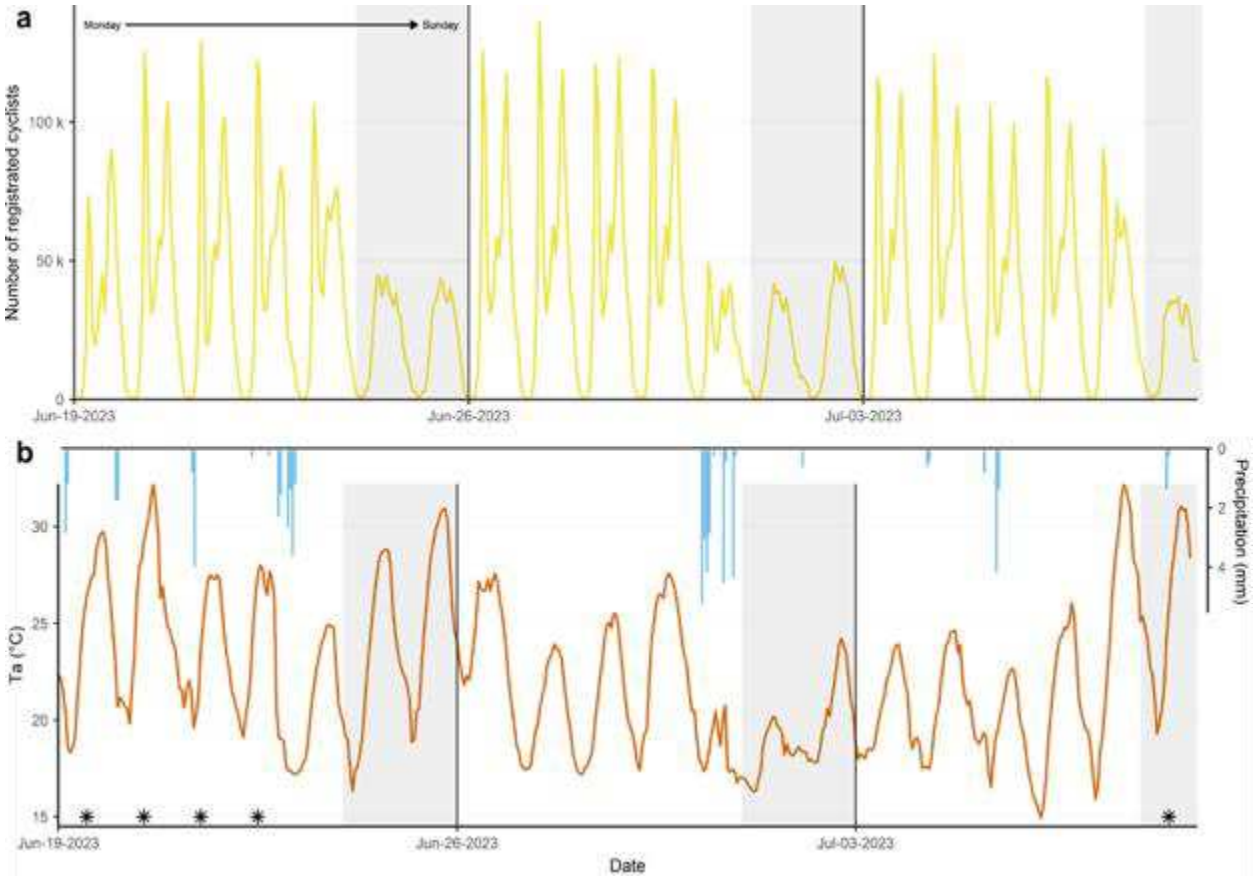


Figure 7: Cycling count data (sum of all segments) (a) and air temperature and precipitation data (b) for the three weeks. The grey shaded areas show weekend days, stars at the bottom of (b) indicate days with official heat warnings by the German Meteorological Service (DWD).

this study are multiplied by a scaling factor $s = 37$ to provide a realistic estimate of the total number of cyclists affected by heat.

4.3 Tree Canopy and Urban Form Data

The tree canopy in Freiburg is available as a digital surface model (DSM) based on airborne Light Detection and Ranging (LiDAR) data, which represents vegetation heights for all trees on public and private land. This DSM is created using a layer that indicates pixels classified as 'tree' in the Briegel et al.[53] land cover dataset. The highest LiDAR[82] return within each pixel covered by a tree is assigned as the canopy height above ground level, while the ground level is calculated as the last return. Pixels not classified as 'tree' are assigned a value of zero. To account for potential artifacts, such as cars, and to ensure that vegetation is sufficiently tall to provide shade, the DSM is filtered to remove values below 2 m above ground level.

4.4 Microclimate and UTCI Modeling

The UTCI modeling is performed using the HTC-NN model of Briegel et al.[53,76]. The HTC-NN is a machine learning-based model that predicts air temperature, humidity, MRT, and wind speed at pedestrian level and at 1 m resolution, with hourly temporal resolution, allowing the calculation of UTCI. The model has been extensively evaluated using numerical models and measurement data from a sensor network in Freiburg, Germany. It is accurate, with an overall MAE of 2.3 K compared with similar numerical models and measurement data[14]. The HTC-NN enables rapid estimation of UTCI maps for entire cities over long time periods[18]. The model uses building and vegetation structures and land cover classes as spatial input data, and air temperature, humidity, downward short- and longwave radiation, wind speed, and direction as meteorological forcing data. The forcing data are provided by a meteorological station located on a rooftop in Freiburg's city center (about 55 m a.g.l.). More details on the model development, testing, evaluation, and its input data can be found here[53,76].

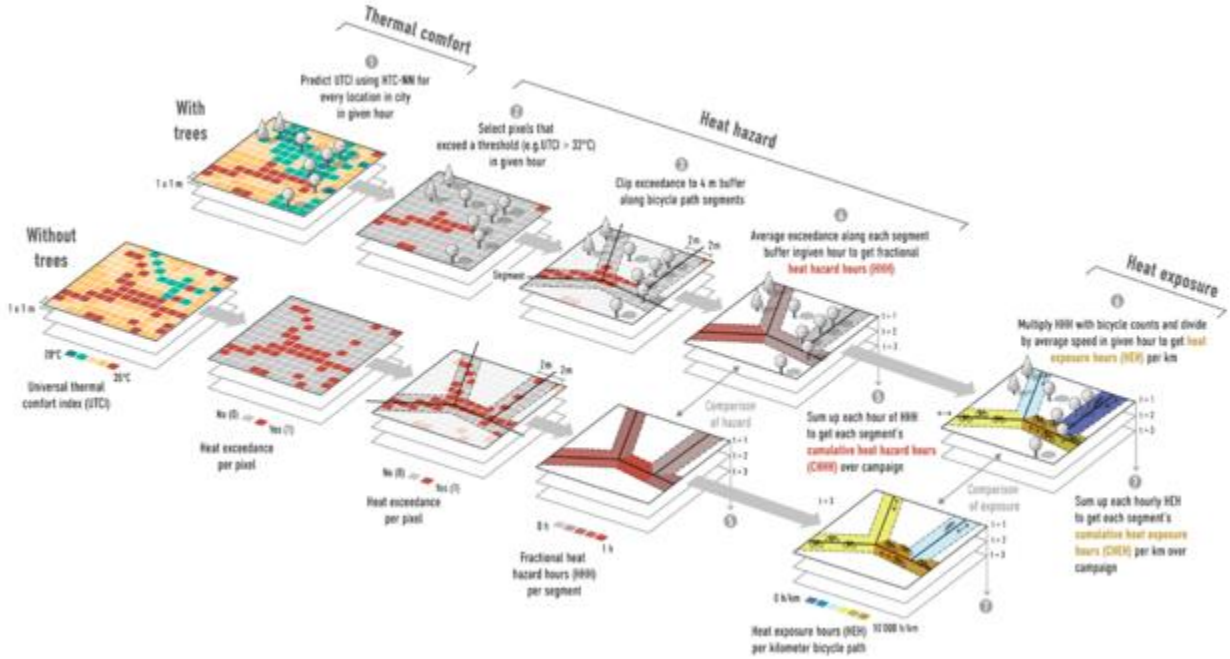


Figure 8: Working procedure involving the modeling of thermal comfort at 1 x 1 m resolution for each hour (1), the identification of heat hazard (2 to 5), and the calculation of heat exposure along the bicycle lane segments (6 and 7). The procedure is run in a first simulation with all current trees included (back row) and in a second simulation, removing all current trees (front row) to compare and therefore assess the cooling potential of current trees. See text for a detailed description.

This study applies the HTC-NN model to two different scenarios. The first scenario represents the actual structure of buildings and vegetation in Freiburg. The second scenario removes all public and private trees from the spatial input data to evaluate the contribution of existing tree canopy to cyclists' heat exposure. Importantly, the no-tree scenario is not implemented only as a geometric change in the DSM or as a simple removal of shade. Instead, scenario-specific meteorological forcing fields are generated using the Surface Urban Energy and Water Balance Scheme (SUEWS). Thus, removing trees affects both the radiative environment through changes in obstruction and shading and the near-surface atmospheric conditions through changes in the surface energy balance, evapotranspiration, storage heat fluxes, and turbulent exchange. These scenario-specific outputs are then used as meteorological forcing for the HTC-NN model, together with the corresponding building, vegetation, and land-cover inputs. In both scenarios, UTCI is modeled for the 20-day period from 2023-06-19 to 2023-07-08.

4.5 Data Analysis

To assess not only heat hazard but also heat exposure among cyclists, mobility data from the 'STADTRADELN' campaign is combined with high-resolution UTCI maps. A detailed flowchart of the data processing is shown in Figure 8.

4.5.1 Cumulative Heat Hazard Hours

In the first step, hourly UTCI maps are calculated for the entire city of Freiburg using the HTC-NN (Figure 8, Step 1). In a second step, a heat exceedance mask is derived from the hourly UTCI maps. This hourly exceedance mask identifies pixels in each hour whose UTCI values exceed a given threshold, such as 26 °C or 32 °C, indicating at least moderate or strong heat stress, respectively (Figure 8, Step 2). In a third step, the binary heat-exceedance mask for a given threshold is assigned to bicycle segments. A 2 m lateral buffer is applied to all linear segments to represent the typical 4 m width of cycling paths, meaning each segment covers an area roughly four times its length (Figure 8, Step 3). Then, the average fractional *heat hazard hours* (HHH) for each segment are calculated by averaging all pixels within the buffer from the binary heat exceedance mask. These fractional HHH represent the hourly average period of strong heat stress (or more), ranging from 0 hours (no pixels above the threshold) to 1 hour (all pixels above the threshold). Summing up all hourly HHH values over the three weeks gives the *cumulative heat hazard hours* (CHHH, in h) (Figure 8, Step 5). The CHHH metric enables spatial analysis of heat frequency over a longer period along cycling paths, regardless of timing or the number of cyclists affected.

4.5.2 Cumulative Heat Exposure Hours

To assess actual cyclist exposure, the final step is to merge the hourly HHH data with cyclist counts and speeds to estimate actual heat exposure (Figure 8, Step 6). As the 'STADTRADELN' dataset contains information not only on the cycling pathways themselves but also on the total number of participants, the average speed, and the number of logs per hour and per segment, it is possible to estimate the actual heat exposure of mobile cyclists as a function of frequency and cycling speed (Figure 8, Step 6). To achieve this, HHH of each segment is divided by the average cyclist speed (v, km h^{-1}) and multiplied by the number

of logs (N, dimensionless) per hour to calculate the actual *heat exposure hours* (HEH) per km (in h km^{-1}). These values are then multiplied by the scaling factor s = 37, as the impact on cyclists is likely to be around 37 times greater than the results estimated from the 'STADTRADELN' campaign alone (see Section 2.2).

$$HEH = \frac{HHH \cdot N \cdot s}{v} \quad (1)$$

The HEH values incorporate time information on how long it takes cyclists to pass through each segment. This allows the total HEH per km for all logs within each hour to be calculated. Thus, HEH enables an analysis of the actual heat exposure in each hour. For example, the HEH is lower for a segment with few cyclists than for one with many cyclists (assuming the remaining parameters remain constant). Since the nocturnal log count is often 0, only records between 08:00 h and 22:00 h CET are used for further analysis. Summing all the HEH values for a segment across the entire campaign yields *cumulative heat exposure hours* (CHEH) (Figure 8, Step 7).

4.6 Role of Shade from Trees and Urban Infrastructure

To quantify the influence of the surrounding urban structure on heat hazard and exposure, the amount of tree and building cover is calculated for each cycling segment. These metrics characterize the local urban morphology and land cover and relate CHHH and CHEH to the combined influence of vegetation and built structures. To this end, a 20 m spatial buffer is applied to both sides of each segment, resulting in an effective corridor width of 40 m along the segment length. This two-sided segment buffer was used to capture the local land-cover and urban-form conditions surrounding each cycling path, including trees, buildings, and surface characteristics that influence shortwave and longwave radiative exchange at cyclist height. Because near-ground thermal exposure is strongly controlled by surface radiation and air temperature, these adjacent land-use characteristics are implicitly represented in the HTC-NN input layers and in the segment-level tree and building cover metrics. Within the 20 m buffer, tree canopy cover and the building plan area ratio are calculated for each segment based on respective spatial datasets. Tree canopy cover is derived from the tree canopy layer described above, while building cover is calculated from

building footprint data. These fractions represent the proportion of the buffered area occupied by tree canopy and building footprints, respectively.

Data availability

Forcing, spatial, and heat stress data will be made available upon request.

Acknowledgments

This research was funded by a Stihl Stiftung Fellowship to AM to visit the Faculty of Environment and Natural Resources at the University of Freiburg. AM received further support from the National Science Foundation under grant CMMI-1942805 (CAREER: Human Thermal Exposure in Cities - Novel Sensing and Modeling to Build Heat-Resilience). FB is funded by the Helmholtz program "Changing Earth" at KIT. AC received funding for this work from the European Commission under ERC Synergy "urbisphere" (Grant Agreement 855005) and from the European Union under "UrbanAir" (Grant Agreement 101188131). Any opinions, findings, conclusions, or recommendations expressed in this material are those of the authors and do not necessarily reflect the views of the sponsoring organizations.

References

1. Nazarian, N. *et al.* Integrated Assessment of Urban Overheating Impacts on Human Life. *Earths Future* **10**, e2022EF002682 (2022).
2. Seneviratne, S. I. *et al.* Weather and Climate Extreme Events in a Changing Climate. in *Climate Change 2021: The Physical Science Basis. Contribution of Working Group I to the Sixth Assessment Report of the Intergovernmental Panel on Climate Change* (eds. Masson-Delmotte, V. et al.) 1513–1766 (Cambridge University Press, Cambridge, United Kingdom and New York, NY, USA, 2021). doi:10.1017/9781009157896.013.
3. Oke, T. R. The energetic basis of the urban heat island. *Quarterly Journal of the Royal Meteorological Society* **108**, 1–24 (1982).
4. Li, D. & Bou-Zeid, E. Synergistic Interactions between Urban Heat Islands and Heat Waves: The Impact in Cities Is Larger than the Sum of Its Parts. *J. Appl. Meteorol. Climatol.* **52**, 2051–2064 (2013).
5. Cissé, G. *et al.* Health, Wellbeing, and the Changing Structure of Communities. in *Climate Change 2022: Impacts, Adaptation and Vulnerability. Contribution of Working Group II to the Fifth Assessment Report of the Intergovernmental Panel on Climate Change.* (eds. Pörtner, H.-O. et al.) 1041–1170 (Cambridge University Press, Cambridge, UK and New York, NY, USA, 2022). doi:10.1017/9781009325844.009.
6. Höppe, P. A new procedure to determine the mean radiant temperature outdoors. *Wetter und Leben* **44**, 147–151 (1992).
7. Middel, A. & Krayenhoff, E. S. Micrometeorological determinants of pedestrian thermal exposure during record-breaking heat in Tempe, Arizona: Introducing the MaRTy observational platform. *Science of the Total Environment* **687**, 137–151 (2019).
8. Höppe, P. The physiological equivalent temperature – A universal index for the biometeorological assessment of the thermal environment. *Int. J. Biometeorol.* **43**, 71–75 (1999).
9. Blazejczyk, K., Epstein, Y., Jendritzky, G., Staiger, H. & Tinz, B. Comparison of UTCI to selected thermal indices. *Int. J. Biometeorol.* **56**, 515–535 (2012).
10. Epstein, Y. & Moran, D. S. Thermal Comfort and the Heat Stress Indices. *Ind. Health* **44**, 388–398 (2006).

11. de Freitas, C. R. & Grigorieva, E. A. A comparison and appraisal of a comprehensive range of human thermal climate indices. *Int. J. Biometeorol.* **61**, 487–512 (2017).
12. Ali-Toudert, F. & Mayer, H. Numerical study on the effects of aspect ratio and orientation of an urban street canyon on outdoor thermal comfort in hot and dry climate. *Build. Environ.* **41**, 94–108 (2006).
13. Buo, I., Sagris, V., Jaagus, J. & Middel, A. High-resolution thermal exposure and shade maps for cool corridor planning. *Sustain. Cities Soc.* **93**, 104499 (2023).
14. Briegel, F., Wehrle, J., Schindler, D. & Christen, A. High-resolution multi-scaling of outdoor human thermal comfort and its intra-urban variability based on machine learning. *Geosci. Model Dev.* **17**, 1667–1688 (2024).
15. Turner, B. L. *et al.* A framework for vulnerability analysis in sustainability science. *Proceedings of the National Academy of Sciences* **100**, 8074–8079 (2003).
16. Ellena, M., Breil, M. & Soriani, S. The heat-health nexus in the urban context: A systematic literature review exploring the socio-economic vulnerabilities and built environment characteristics. *Urban Clim.* **34**, 100676 (2020).
17. Luo, Y., Cheng, X., He, B.-J. & Dewancker, B. J. Identification and assessment of heat disaster risk: a comprehensive framework based on hazard, exposure, adaptation and vulnerability. *International Journal of Environmental Science and Technology* **22**, 11275–11294 (2025).
18. Briegel, F. *et al.* Deep learning enables city-wide climate projections of street-level heat stress. *Urban Clim.* **62**, 102564 (2025).
19. Zahabi, S. A. H., Chang, A., Miranda-Moreno, L. F. & Patterson, Z. Exploring the link between the neighborhood typologies, bicycle infrastructure and commuting cycling over time and the potential impact on commuter GHG emissions. *Transp. Res. D Transp. Environ.* **47**, 89–103 (2016).
20. Neves, A. & Brand, C. Assessing the potential for carbon emissions savings from replacing short car trips with walking and cycling using a mixed GPS-travel diary approach. *Transp. Res. Part A Policy Pract.* **123**, 130–146 (2019).
21. Bean, R., Pojani, D. & Corcoran, J. How does weather affect bikeshare use? A comparative analysis of forty cities across climate zones. *J. Transp. Geogr.* **95**, 103155 (2021).

22. Miranda-Moreno, L. F. & Nosal, T. Weather or Not to Cycle. *Transportation Research Record: Journal of the Transportation Research Board* **2247**, 42–52 (2011).
23. Wessel, J. Using weather forecasts to forecast whether bikes are used. *Transp. Res. Part A Policy Pract.* **138**, 537–559 (2020).
24. Tin Tin, S., Woodward, A., Robinson, E. & Ameratunga, S. Temporal, seasonal and weather effects on cycle volume: an ecological study. *Environmental Health* **11**, 12 (2012).
25. Moser, M. K. *et al.* Understanding the influence of urban characteristics on cyclists' stress measured through wearable sensors: A quantitative open data approach. *Environ. Plan. B Urban Anal. City Sci.* **53**, 336–362 (2026).
26. Ermagun, A., Lindsey, G. & Loh, T. H. Urban trails and demand response to weather variations. *Transp. Res. D Transp. Environ.* **63**, 404–420 (2018).
27. Heaney, A. K., Carrión, D., Burkart, K., Lesk, C. & Jack, D. Climate change and physical activity: Estimated impacts of ambient temperatures on bikeshare usage in new york city. *Environ. Health Perspect.* **127**, 037002-1-037002–10 (2019).
28. Buo, I. *et al.* Cool routes: Real-time human thermal exposure routing. *Build. Environ.* **298**, (2026).
29. Helbich, M., Böcker, L. & Dijst, M. Geographic heterogeneity in cycling under various weather conditions: evidence from Greater Rotterdam. *J. Transp. Geogr.* **38**, 38–47 (2014).
30. Young, E. *et al.* Modeling outdoor thermal comfort along cycling routes at varying levels of physical accuracy to predict bike ridership in Cambridge, MA. *Build. Environ.* **208**, 108577 (2022).
31. Schmitt, A. U. *et al.* Assessing the weather conditions for urban cyclists by spatially dense measurements with an agent-based approach. *Meteorological Applications* **30**, (2023).
32. Cao, B., Sun, M. & Bardhan, R. Measuring shaded bike lanes for heat stress mitigation with deep learning: A case study in Amsterdam, Netherlands. *Urban Clim.* **57**, 102126 (2024).
33. Huang, J. & Fang, C. Does shadow matter? Exploring the influence of shade provision on cycling activity from the perspective of urban climate resilience. *Sustain. Cities Soc.* **136**, 107103 (2026).
34. Li, R. *et al.* Effectiveness of travel behavior and infrastructure change to mitigate heat exposure. *Frontiers in Sustainable Cities* **5**, 13 (2023).

35. Li, R. *et al.* Repurposing mesoscale traffic models for insights into traveler heat exposure. *Transp. Res. D Transp. Environ.* **114**, 103548 (2023).
36. Fünfgeld, H. *et al.* Optimizing urban greening and densification in the context of outdoor heat: Opportunities for AI-supported urban adaptation. *Landsc. Urban Plan.* **268**, 105574 (2026).
37. Aminipouri, M. *et al.* Urban tree planting to maintain outdoor thermal comfort under climate change: The case of Vancouver's local climate zones. *Build. Environ.* **158**, 226–236 (2019).
38. Aminipouri, M., Knudby, A. J., Krayenhoff, E. S., Zickfeld, K. & Middel, A. Modelling the impact of increased street tree cover on mean radiant temperature across Vancouver's local climate zones. *Urban For. Urban Green.* **39**, 9–17 (2019).
39. Middel, A., Selover, N., Hagen, B. & Chhetri, N. Impact of shade on outdoor thermal comfort—a seasonal field study in Tempe, Arizona. *Int. J. Biometeorol.* **60**, 1849–1861 (2016).
40. Middel, A., AlKhaled, S., Schneider, F. A., Hagen, B. & Coseo, P. 50 Grades of Shade. *Bull. Am. Meteorol. Soc.* **102**, E1805–E1820 (2021).
41. Coutts, A. M., White, E. C., Tapper, N. J., Beringer, J. & Livesley, S. J. Temperature and human thermal comfort effects of street trees across three contrasting street canyon environments. *Theor. Appl. Climatol.* **124**, 55–68 (2016).
42. Holst, J. & Mayer, H. Impacts of street design parameters on human-biometeorological variables. *Meteorologische Zeitschrift* **20**, 241–552 (2011).
43. Middel, A., Chhetri, N. & Quay, R. Urban forestry and cool roofs: Assessment of heat mitigation strategies in Phoenix residential neighborhoods. *Urban For. Urban Green.* **14**, 178–186 (2015).
44. Li, H. *et al.* Cooling efficacy of trees across cities is determined by background climate, urban morphology, and tree trait. *Commun. Earth Environ.* **5**, 754 (2024).
45. Middel, A., Nazarian, N., Demuzere, M. & Bechtel, B. Urban Climate Informatics: An Emerging Research Field. *Front. Environ. Sci.* **10**, 532 (2022).
46. Briegel, F., Makansi, O., Brox, T., Matzarakis, A. & Christen, A. Modelling long-term thermal comfort conditions in urban environments using a deep convolutional encoder-decoder as a computational shortcut. *Urban Clim.* **47**, 101359 (2023).

47. STADTRADELN. STADTRADELN 2023, Freiburg im Breisgau. https://www.stadtradeln.de/freiburg (2026).
48. Turner, B. L. *et al.* A framework for vulnerability analysis in sustainability science. *Proc. Natl. Acad. Sci. U. S. A.* **100**, 8074–8079 (2003).
49. Ellena, M., Breil, M. & Soriani, S. The heat-health nexus in the urban context: A systematic literature review exploring the socio-economic vulnerabilities and built environment characteristics. *Urban Clim.* **34**, 100676 (2020).
50. Luo, Y., Cheng, X., He, B. J. & Dewancker, B. J. Identification and assessment of heat disaster risk: a comprehensive framework based on hazard, exposure, adaptation and vulnerability. *International Journal of Environmental Science and Technology 2024 22:12* **22**, 11275–11294 (2024).
51. Ali-Toudert, F. & Mayer, H. Numerical study on the effects of aspect ratio and orientation of an urban street canyon on outdoor thermal comfort in hot and dry climate. *Build. Environ.* **41**, 94–108 (2006).
52. Buo, I., Sagris, V., Jaagus, J. & Middel, A. High-resolution thermal exposure and shade maps for cool corridor planning. *Sustain. Cities Soc.* **93**, 104499 (2023).
53. Briegel, F., Wehrle, J., Schindler, D. & Christen, A. High-resolution multi-scaling of outdoor human thermal comfort and its intra-urban variability based on machine learning. *Geosci. Model Dev.* **17**, (2024).
54. Miranda-Moreno, L. & Nosal, T. Weather or not to cycle: Temporal trends and impact of weather on cycling in an urban environment. *Transp. Res. Rec.* 42–52 (2011) doi:10.3141/2247-06;REQUESTEDJOURNAL:JOURNAL:TRRA;PAGE:STRING:ARTICLE/CHAPTER.
55. Tin Tin, S., Woodward, A., Robinson, E. & Ameratunga, S. Temporal, seasonal and weather effects on cycle volume: an ecological study. *Environmental Health 2012 11:1* **11**, 12- (2012).
56. Ermagun, A., Lindsey, G. & Loh, T. H. Urban trails and demand response to weather variations. *Transp. Res. D Transp. Environ.* **63**, 404–420 (2018).
57. Heaney, A. K., Carrión, D., Burkart, K., Lesk, C. & Jack, D. Climate Change and Physical Activity: Estimated Impacts of Ambient Temperatures on Bikeshare Usage in New York City. *Environ. Health Perspect.* **127**, 037002-1-037002–10 (2019).

58. Wessel, J. Using weather forecasts to forecast whether bikes are used. *Transp. Res. Part A Policy Pract.* **138**, 537–559 (2020).
59. Bean, R., Pojani, D. & Corcoran, J. How does weather affect bikeshare use? A comparative analysis of forty cities across climate zones. *J. Transp. Geogr.* **95**, 103155 (2021).
60. Cao, B., Sun, M. & Bardhan, R. Measuring shaded bike lanes for heat stress mitigation with deep learning: A case study in Amsterdam, Netherlands. *Urban Clim.* **57**, 102126 (2024).
61. Huang, J. & Fang, C. Does shadow matter? Exploring the influence of shade provision on cycling activity from the perspective of urban climate resilience. *Sustain. Cities Soc.* **136**, 107103 (2026).
62. Li, R. *et al.* Repurposing mesoscale traffic models for insights into traveler heat exposure. *Transp. Res. D Transp. Environ.* **114**, 103548 (2023).
63. Li, R. *et al.* Effectiveness of travel behavior and infrastructure change to mitigate heat exposure. *Frontiers in Sustainable Cities* **5**, 13 (2023).
64. Middel, A., Selover, N., Hagen, B. & Chhetri, N. Impact of shade on outdoor thermal comfort—a seasonal field study in Tempe, Arizona. *Int. J. Biometeorol.* **60**, 1849–1861 (2016).
65. Aminipouri, M., Knudby, A. J., Krayenhoff, E. S., Zickfeld, K. & Middel, A. Modelling the impact of increased street tree cover on mean radiant temperature across Vancouver's local climate zones. *Urban For. Urban Green.* **39**, (2019).
66. Middel, A., AlKhaled, S., Schneider, F. A., Hagen, B. & Coseo, P. 50 Grades of Shade. *Bull. Am. Meteorol. Soc.* 1–35 (2021) doi:10.1175/bams-d-20-0193.1.
67. Aminipouri, M. *et al.* Urban tree planting to maintain outdoor thermal comfort under climate change: The case of Vancouver's local climate zones. *Build. Environ.* **158**, (2019).
68. Coutts, A. M., White, E. C., Tapper, N. J., Beringer, J. & Livesley, S. J. Temperature and human thermal comfort effects of street trees across three contrasting street canyon environments. *Theor. Appl. Climatol.* **124**, 55–68 (2016).
69. Li, H. *et al.* Cooling efficacy of trees across cities is determined by background climate, urban morphology, and tree trait. *Commun. Earth Environ.* **5**, 754 (2024).
70. Fünfgeld, H. *et al.* Optimizing urban greening and densification in the context of outdoor heat: Opportunities for AI-supported urban adaptation. *Landsc. Urban Plan.* **268**, 105574 (2026).

71. Holst, J. & Mayer, H. Impacts of street design parameters on human-biometeorological variables. *Meteorologische Zeitschrift* **20**, 541–552 (2011).
72. Zahabi, S. A. H., Chang, A., Miranda-Moreno, L. F. & Patterson, Z. Exploring the link between the neighborhood typologies, bicycle infrastructure and commuting cycling over time and the potential impact on commuter GHG emissions. *Transp. Res. D Transp. Environ.* **47**, 89–103 (2016).
73. Neves, A. & Brand, C. Assessing the potential for carbon emissions savings from replacing short car trips with walking and cycling using a mixed GPS-travel diary approach. *Transp. Res. Part A Policy Pract.* **123**, 130–146 (2019).
74. Middel, A., Nazarian, N., Demuzere, M. & Bechtel, B. Urban Climate Informatics: An Emerging Research Field. *Front. Environ. Sci.* **10**, 532 (2022).
75. (IPCC), I. P. on C. C. Health, Wellbeing and the Changing Structure of Communities. *Climate Change 2022 – Impacts, Adaptation and Vulnerability* 1041–1170 (2023) doi:10.1017/9781009325844.009.
76. Briegel, F., Makansi, O., Brox, T., Matzarakis, A. & Christen, A. Modelling long-term thermal comfort conditions in urban environments using a deep convolutional encoder-decoder as a computational shortcut. *Urban Clim.* **47**, 101359 (2023).
77. DWD Climate Data Center (CDC). Multi-annual station means for the climate normal reference period 1991-2020, for current station location and for reference station location. https://opendata.dwd.de/climate_environment/CDC/observations_germany/climate/ (2026).
78. Plein, M., Feigel, G., Zeeman, M., Dormann, C. F. & Christen, A. Using Gradient Boosting for gap-filling to analyze temperature and humidity patterns in an urban weather station network in Freiburg, Germany. *Urban Clim.* **62**, 102496 (2025).
79. Hundhausen, M., Feldmann, H., Laube, N. & Pinto, J. G. Future heat extremes and impacts in a convection-permitting climate ensemble over Germany. *Natural Hazards and Earth System Sciences* **23**, 2873–2893 (2023).
80. DWD. DWD: Historische Hitzewarnungen in Deutschland, Version v001, 2021. opendata.dwd.de/climate_environment/health/historical_alerts/heat_warnings/ (2026).
81. Christen, A., Sulzer, M. & Zeeman, M. Air temperature measurements from Automatic Weather Station (AWS) at Freiburg – Werthmannstrasse (FRWRTM) from 2023-01-01 to

2023-12-31 [L2] (1.2) [Dataset]. *University of Freiburg* Preprint at https://doi.org/10.5281/zenodo.1085520 (2025).

82. City of Freiburg im Breisgau. LiDAR dataset [Data set]. Available upon request. Preprint at (2021).

Supplementary Files

This is a list of supplementary files associated with this preprint. Click to download.

- CaseStudy.docx